© 2021. Published by The Company of Biologists Ltd | Journal of Experimental Biology (2021) 224, jeb233544. doi:10.1242/jeb.233544

RESEARCH ARTICLE

Accounting for body mass effects in the estimation of field metabolic rates from body acceleration

Evan E. Byrnes[1,2,3,*], Karissa O. Lear[1], Lauran R. Brewster[3,4], Nicholas M. Whitney[5], Matthew J. Smukall[3,6], Nicola J. Armstrong[1,7] and Adrian C. Gleiss[1,2]

ABSTRACT

Dynamic body acceleration (DBA), measured through animal-attached tags, has emerged as a powerful method for estimating field metabolic rates of free-ranging individuals. Following respirometry to calibrate oxygen consumption rate ($\dot{M}_{O_2}$) with DBA under controlled conditions, predictive models can be applied to DBA data collected from free-ranging individuals. However, laboratory calibrations are generally performed on a relatively narrow size range of animals, which may introduce biases if predictive models are applied to differently sized individuals in the field. Here, we tested the mass dependence of the $\dot{M}_{O_2}$–DBA relationship to develop an experimental framework for the estimation of field metabolic rates when organisms differ in size. We performed respirometry experiments with individuals spanning one order of magnitude in body mass (1.74–17.15 kg) and used a two-stage modelling process to assess the intraspecific scale dependence of the $\dot{M}_{O_2}$–DBA relationship and incorporate such dependencies into the coefficients of $\dot{M}_{O_2}$ predictive models. The final predictive model showed scale dependence; the slope of the $\dot{M}_{O_2}$–DBA relationship was strongly allometric ($M^{1.55}$), whereas the intercept term scaled closer to isometry ($M^{1.08}$). Using bootstrapping and simulations, we evaluated the performance of this coefficient-corrected model against commonly used methods of accounting for mass effects on the $\dot{M}_{O_2}$–DBA relationship and found the lowest error and bias in the coefficient-corrected approach. The strong scale dependence of the $\dot{M}_{O_2}$–DBA relationship indicates that caution must be exercised when models developed using one size class are applied to individuals of different sizes.

KEY WORDS: Lemon shark, *Negaprion brevirostris*, Oxygen consumption rate, Biologging, Ecophysiology, Elasmobranch, Respirometry

INTRODUCTION

Estimating the metabolic rates of animals in the laboratory is a well-established practice using either direct or indirect calorimetry; however, estimating field metabolic rate (FMR) is more challenging. Commonly used methods to estimate FMR include measuring CO_2 production via doubly labelled water (DLW; Speakman, 1997), and measuring heart rate (f_H) or dynamic body acceleration (DBA) as a proxy for oxygen consumption rate ($\dot{M}_{O_2}$). Of these, the DBA technique has come to the fore because of its wide taxonomic applicability, high temporal resolution (in contrast to DLW; Butler et al., 2004) and the logistical simplicity of attaching acceleration data-loggers, as opposed to the invasive surgery required for implantation of heart-rate loggers (Green et al., 2009). Of course, the DBA technique does have its own limitations, such as difficulties measuring the effects of digestion on energy use (reviewed in Wilson et al., 2020; but see Gleiss et al., 2011). Nonetheless, before using DBA to predict FMR, laboratory calibrations are necessary to establish predictive models that relate DBA to $\dot{M}_{O_2}$ (Gleiss et al., 2011; Wilson et al., 2006). Such calibrations have been conducted for numerous vertebrate and invertebrate species and show that a linear relationship between $\dot{M}_{O_2}$ and DBA holds across all taxa, where the intercept constitutes the baseline (i.e. basal or standard) metabolic rate (BMR) and the slope indicates how $\dot{M}_{O_2}$ changes with activity (Wilson et al., 2020). After appropriate calibrations, predictive models can then be applied to field-measured DBA data to predict the FMR of free-ranging animals.

To discern the utility of any given FMR estimation method, it is necessary to test its sensitivity to factors that are expected to influence $\dot{M}_{O_2}$ and to incorporate appropriate corrections into estimations. For instance, temperature and body size are considered the most important factors that influence metabolism, among other factors (e.g. age, sexual maturity, specific dynamic action), with both displaying positive exponential effects on $\dot{M}_{O_2}$ in ectotherms (Clarke and Johnston, 1999; Gillooly et al., 2001). As temperature is easily manipulated under laboratory conditions, the temperature dependence of the $\dot{M}_{O_2}$–DBA relationship has been tested by numerous studies. As such, it is known that the intercept of the $\dot{M}_{O_2}$–DBA relationship changes with temperature according to a van't Hoff or Arrhenius relationship, while the slope is unaffected (e.g. Lear et al., 2017; Lyons et al., 2013). Accordingly, temperature variation can be accounted for by incorporating a temperature-dependent intercept term into predictive $\dot{M}_{O_2}$ models. Although the level of temperature dependence varies between species, this type of correction has proven to be effective across ectothermic taxa, including fish (Lear et al., 2017, 2020; Wright et al., 2014), reptiles (Enstipp et al., 2011), crustaceans (Lyons et al., 2013) and molluscs (Robson et al., 2016).

Unlike temperature, it is unknown how body size affects the $\dot{M}_{O_2}$–DBA relationship, owing to ethical and logistical difficulties associated with conducting respirometry experiments on large individuals (Whitney et al., 2018). Consequently, calibration experiments have often been limited to individuals spanning relatively narrow ranges in body sizes, which do not fully represent the size range of individuals likely to be encountered

[1]Centre for Sustainable Aquatic Ecosystems, Harry Butler Institute, Murdoch University, 90 South St., Murdoch, WA 6150, Australia. [2]College of Science, Health, Engineering and Education, Murdoch University, 90 South Street, Murdoch, WA 6150, Australia. [3]Bimini Biological Field Station Foundation, South Bimini, Bahamas. [4]Harbor Branch Oceanographic Institute, Florida Atlantic University, 5600 N US Highway 1, Fort Pierce, FL 34946, USA. [5]Anderson Cabot Center for Ocean Life, New England Aquarium, 1 Central Wharf, Boston, MA 02110, USA. [6]College of Fisheries and Ocean Sciences, University of Alaska Fairbanks, 2150 Koyukuk Drive, Fairbanks, AK 99775, USA. [7]Department of Mathematics and Statistics, Curtin University, Kent Street, Bentley, Perth, WA 6102, Australia.

*Author for correspondence (evan.byrnes@murdoch.edu.au)

E.E.B., 0000-0001-7116-246X; K.O.L., 0000-0002-2648-8564; L.R.B., 0000-0002-9798-4370; M.J.S., 0000-0003-3790-3644; N.J.A., 0000-0002-4477-293X; A.C.G., 0000-0002-9960-2858

Received 24 July 2020; Accepted 21 January 2021

Journal of Experimental Biology (2021) 224, jeb233544. doi:10.1242/jeb.233544

when conducting tagging studies in the field (e.g. Lear et al., 2020; Watanabe et al., 2019). However, it is likely important that body mass effects are incorporated into estimations of $\dot{M}_{O_2}$, given the well-established allometric scaling patterns of BMR (da Silva et al., 2006; Kleiber, 1932). Defined by a power law:

$$\text{BMR} = aM^b, \quad (1)$$

the BMR of organisms increases positively with body mass (M) at a rate defined by a species-specific scaling coefficient (a) and exponent (b) (White et al., 2007). Thus, given that the intercept of the $\dot{M}_{O_2}$–DBA relationship is representative of BMR, it is expected that the $\dot{M}_{O_2}$–DBA intercept should scale allometrically with body mass.

While there is a reasonably well-defined hypothesis for the allometry of BMR, the kinematics that define animal movement and acceleration, and therefore govern the slope of the $\dot{M}_{O_2}$–DBA relationship, adhere to a different set of allometric laws. For example, physiological forces that govern variations in BMR could relate to factors such as fractal oxygen-transport networks or body surface area to volume ratios, which control the supply of metabolic substrates, and scale at allometric rates near 0.75 (West et al., 1997) and 0.67 (Kozłowski et al., 2003; West and Brown, 2005), respectively. In contrast, DBA is a product of body kinematics, such as stride frequency and amplitude, which scale at allometric rates of approximately −0.33 (Bale et al., 2014) and 0.33 (Videler, 1993), respectively. Furthermore, the fact that active metabolism (i.e. routine and maximum metabolic rate) has been found to scale at a different rate than BMR in all taxa (Bishop, 1999; Killen et al., 2007) suggests that the slope of the $\dot{M}_{O_2}$–DBA relationship, which is representative of energy expenditure due to activity, follows a fundamentally different allometric relationship than BMR. Nonetheless, current methods account for the effects of body mass by applying either isometric (Bouyoucos et al., 2017; O_2 kg^{-1}, e.g. Payne et al., 2011) or allometric (O_2 kg^{-b}, e.g. Enstipp et al., 2011; Lear et al., 2020) mass corrections to $\dot{M}_{O_2}$ estimates, where b is a species-specific BMR scaling exponent. Alternatively, some studies have accounted for effects of mass by simply including body size as a continuous covariate (with no interactions) when modelling the influence of DBA on $\dot{M}_{O_2}$ (e.g. Brownscombe et al., 2017). The former approach assumes an identical $\dot{M}_{O_2}$–DBA slope and intercept mass scaling, whereas the latter approach assumes no effect of mass on the $\dot{M}_{O_2}$–DBA slope. However, if the $\dot{M}_{O_2}$–DBA slope was to scale allometrically at a different rate than BMR, it is likely that these methods introduce significant bias into $\dot{M}_{O_2}$ estimates.

The present study set out to test the effect of mass on both the slope and intercept of the intraspecific $\dot{M}_{O_2}$–DBA relationship and to assess the accuracy of different approaches for incorporating mass effects into $\dot{M}_{O_2}$ predictive models for a species. To do this, we conducted respirometry experiments on individuals spanning one order of magnitude in body mass (1.74–17.15 kg), using lemon sharks (*Negaprion brevirostris*) as a model species. We then used a two-stage modelling process to test for independent mass scaling of the intercept and slope of the $\dot{M}_{O_2}$–DBA relationship. We incorporated the established mass-scaling effects into the coefficients of $\dot{M}_{O_2}$ predictive models and compared this model against other commonly used modelling approaches through a series of simulations that allowed assessment of the biases and error associated with each model.

MATERIALS AND METHODS

Capture and maintenance

Respirometry experiments were conducted on two groups of lemon sharks [*Negaprion brevirostris* (Poey 1868)]. The first group consisted of individuals <3 kg in mass [n=16, 69.5–86.0 cm total length (TL)], captured off Florida, USA, and housed at Mote Marine Laboratory (MML) in Sarasota, FL, USA, for the duration of experiments. Further capture and maintenance details for MML individuals are provided in Lear et al. (2017). The second group consisted of individuals >3 kg in mass (n=5, 107.0–154.0 cm TL), captured and housed in semi-captive pens off South Bimini, Bahamas, near Bimini Biological Field Station (BBFS), where they were subjected to natural environmental conditions (e.g. temperature, light and salinity). All sharks were fasted for at least 48 h prior to experiments to ensure a post-absorptive state and allow recovery from capture stress.

Research was conducted under permits from the Bahamas Department of Marine Resources (MA&MR/FIS/178), Murdoch University Animal Ethics (RW3119/19) and Mote Marine Laboratory Institutional Animal Care and Use Committee (09-09-NW1).

Respirometry trial protocol

For MML sharks, respirometry was conducted between 2015 and 2016 as part of a separate study (Lear et al., 2017). A closed, annular, static respirometry system was constructed from a modified 2.45 m diameter fibreglass holding tank, as described in Whitney et al. (2016). Sharks were acclimated to the system for 12 h prior to trials. Trials began near 100% air saturation and were run until dissolved oxygen (DO) levels reached 80% air saturation. DO (% air saturation and mg l^{-1}) and water temperature (°C) were measured by a handheld multiparameter meter (Pro Plus, Yellow Springs Instruments, Yellow Springs, OH, USA) and recorded by researchers every 5 min throughout trials. To assess background respiration, a blank respirometer was measured for 4 h following each set of trials. For full details of the MML trial protocol, see Lear et al. (2017).

BBFS trials were conducted using a field-based respirometry system, similar to Byrnes et al. (2020). Two closed, annular, static respirometry systems were constructed from modified polyvinyl-lined metal-frame pools (Bestway Corp., London, UK), which were erected on a levelled section of beach on South Bimini, Bahamas. A 2.44 m diameter pool was used for sharks <110 cm TL, whereas a 3.66 m diameter pool was used for sharks >110 cm TL. Sharks were hand-netted from pens, measured and weighed, and transferred into the system 8 h prior to trials to allow them to acclimate. Trials began with air saturation between 80 and 110% and were run until saturation decreased by 20 percentage points or reached 70% saturation, whichever occurred first. Throughout trials, DO (% air saturation and mg l^{-1}) and water temperature (°C) were measured and recorded by a multiparameter meter (HI98196, Hanna Instruments, RI, USA) every 30 s. To assess background respiration, a blank respirometer was measured for at least 90 min immediately following the final trial for each shark.

Throughout all MML and BBFS trials, sharks were equipped with a Cefas G6a+ acceleration data logger (Cefas Inc., Lowestoft, UK), mounted through the base of the first dorsal fin as per Lear et al. (2017), which continuously recorded triaxial acceleration at 25 Hz (range: 2 g, resolution: 12-bit).

Body acceleration and oxygen consumption rate estimation

Vectorial dynamic body acceleration (VeDBA), a measurement of physical activity, was calculated from acceleration data recorded

Journal of Experimental Biology (2021) 224, jeb233544. doi:10.1242/jeb.233544

during respirometry. VeDBA was chosen as the acceleration metric for modelling instead of the commonly used overall dynamic body acceleration to allow predictive models to be applied to data collected by acceleration transmitters (see www.innovasea.com/fish-tacking/ for various applications), which process acceleration onboard as VeDBA. Additionally, VeDBA produces more robust estimations of activity when tag orientation may differ between applications, such as external mounting of loggers versus internal implantation of transmitters (Qasem et al., 2012).

To match the sampling frequency of acceleration transmitters, which record long-term field data at 5 Hz, raw acceleration data were down-sampled by decimation from 25 to 5 Hz, which has been shown to be a sufficient sampling frequency for estimating oxygen consumption rates of fishes (Brownscombe et al., 2018). As per the algorithm used by acceleration transmitters (e.g. Vemco V13AP, Innovasea Systems Inc., Nova Scotia, Canada), gravitational acceleration was estimated by calculating a 4 s running mean. Gravitational acceleration was then subtracted from the raw acceleration, for each axis, to derive DBA. VeDBA was calculated as the vectorial sum of these DBA derivations:

$$\text{VeDBA} = \sqrt{(A_{X_t} - G_{X_t})^2 + (A_{Y_t} - G_{Y_t})^2 + (A_{Z_t} - G_{Z_t})^2}, \quad (2)$$

where A_{X_t}, A_{Y_t} and A_{Z_t} are the raw acceleration values and G_{X_t}, G_{Y_t} and G_{Z_t} are the gravitational acceleration values observed for each axis at time t. Acceleration data were processed using Igor Pro (Version 7.08; Wavemetrics, Lake Oswego, OR, USA) and the Ethographer extension (Sakamoto et al., 2009).

Dynamic acceleration data were visually examined to identify intervals where sharks maintained consistent resting (i.e. inactive) or swimming (i.e. active) behaviour for 15–20 min during trials. Higher sampling frequencies of DO used during BBFS than MML trials allowed for shorter calibration intervals to be used for BBFS trials. Therefore, intervals of at least 20 min were used for MML sharks (Lear et al., 2017), whereas intervals of 15 min were used for BBFS sharks to increase the number of individual estimates of oxygen consumption rate for BBFS trials. Mean water temperature, VeDBA and whole-animal oxygen consumption rate ($\dot{M}_{O_2\text{whole}}$; mg O_2 h^{-1}) were calculated for each interval. $\dot{M}_{O_2\text{whole}}$ was calculated using the following equation from measurements of DO within respirometers:

$$\dot{M}_{O_2\text{whole}} = (R_{\text{total}} - R_{\text{background}} + d) \cdot 60 \cdot \left(V_r - \frac{M}{p}\right), \quad (3)$$

where R_{total} is the rate of decline of DO during the calibration interval (mg O_2 l^{-1} min^{-1}; estimated using linear regression), $R_{\text{background}}$ is the rate of background respiration (mg O_2 l^{-1} min^{-1}), d is the diffusion rate of oxygen into the system (0.0002 mg O_2^{-1} l^{-1} min^{-1}; Byrnes et al., 2020), V_r is the respirometer volume (l), M is the mass of the shark (kg) and p is the density of the shark (kg l^{-1}). All sharks were assumed to have a density of 1.0556 kg l^{-1}, the average density reported for adult *N. brevirostris* in Florida (Baldridge, 1970).

To remove variation in oxygen consumption rates due to temperature, all $\dot{M}_{O_2\text{whole}}$ estimations were temperature corrected to 29.5°C, the mean water temperature of MML trials, using:

$$\dot{M}_{O_2\text{whole},29.5} = \dot{M}_{O_2\text{whole,a}} \times Q_{10}^{(29.5-T_a)/10}, \quad (4)$$

where $\dot{M}_{O_2\text{whole},29.5}$ is the $\dot{M}_{O_2\text{whole}}$ calculated at 29.5°C, $\dot{M}_{O_2\text{whole,a}}$ is the measured $\dot{M}_{O_2\text{whole}}$, T_a is the temperature at which $\dot{M}_{O_2\text{whole,a}}$ was measured, and Q_{10} is the temperature scaling factor for lemon sharks. A Q_{10} of 2.96 was used to correct $\dot{M}_{O_2\text{whole,a}}$ during inactive intervals, and a Q_{10} of 1.69 was used to correct $\dot{M}_{O_2\text{whole,a}}$ during active intervals (Lear et al., 2017).

Pre-modelling data processing

Prior to building predictive models, VeDBA estimates were corrected for measurement error (i.e. acceleration irrespective of body movement), to ensure that the model intercept represented SMR of sharks. As previously mentioned, the intercept of the $\dot{M}_{O_2}$–DBA relationship represents zero movement (i.e. maintenance metabolic rate; Wilson et al., 2020); however, owing to factors causing measurement error (e.g. sensor noise, water movement; Gleiss et al., 2010; Whitney et al., 2010), $\dot{M}_{O_2}$ observations during rest tend to be greater than 0***g***. To account for this error, many studies have interpolated to zero movement to estimate SMR (e.g. Lear et al., 2017; Wright et al., 2014); however, such an interpolation likely underestimates SMR. Therefore, to account for measurement error, we rescaled all observations by subtracting the overall mean VeDBA of inactive intervals. Note that while baselining VeDBA in this manner may result in some minorly negative values, this correction was necessary to ensure the intercept was representative of SMR of sharks.

Owing to sharks frequently switching between inactive and active behaviours in MML trials, some sharks only provided one to two $\dot{M}_{O_2\text{whole}}$ observations, precluding the ability to produce a reliable linear fit for each individual body mass (Table 1). To achieve a necessary number of $\dot{M}_{O_2\text{whole}}$ estimations for regressions, MML sharks were grouped into 0.4 kg mass classes (1.60–1.99$\dot{9}$, 2.00–2.39$\dot{9}$, 2.40–2.79$\dot{9}$ and 2.80–3.19$\dot{9}$ kg). The midrange of a class was used as the mass for all sharks within the class during modelling. The BBFS sharks, in contrast, showed a greater range of activity within individual trials and had a larger range in body size, and were therefore kept as individuals rather than grouped into mass classes. We note that this grouping of individuals into mass classes precluded inclusion of ID as a random effect in models, which may have resulted in some degree of pseudoreplication in models, where there are multiple data points per shark.

Testing effect of mass on $\dot{M}_{O_2}$–DBA relationship

To determine the effect of mass on the intercept and slope of the $\dot{M}_{O_2}$–DBA relationship, we conducted a two-stage modelling approach. First, we estimated the relationship between $\dot{M}_{O_2\text{whole}}$ and VeDBA for each mass class of sharks (Fig. 1), described by the linear regression equation:

$$\dot{M}_{O_2\text{whole}} = \beta_i + \beta_s(\text{VeDBA}), \quad (5)$$

where β_i represents the intercept coefficient of the regression and β_s represents the slope coefficient of the regression. To do this, we used a linear mixed-effects model (lme4 package; https://CRAN.R-project.org/package=lme4), which included VeDBA, mass class, and an interaction between VeDBA and mass class as potential covariates to explain variation in $\dot{M}_{O_2\text{whole}}$. Importantly, mass class was included as a categorical variable, which resulted in the mixed-effects model fitting a separate regression for each mass class. The MuMIn package (https://CRAN.R-project.org/package=MuMIn) was used to build models using every combination of explanatory variables and model fit was compared based on Akaike's information criterion (AIC), with decreases in AIC ≥2 considered as improvements in fit (Zuur et al., 2009). Models were fitted with a Gaussian error structure, and model assumptions were checked based on visual examination of residual plots (not shown).

Table 1. Data summary from all respirometry trials

Shark ID	No. of trials	No. of calibration intervals (active/inactive)	Start time (h)	Date	Mean trial duration (h)	Mass (kg)	Mass class	Mean temperature (°C)	Mean $\dot{M}_{O_2whole}$ (mg O_2 h^{-1})
BBFS1*	3	5 (5/0)	20:08	3-May-19	2.23 (1.33–1.52)	14.65	14.65	28.40 (27.32–30.02)	5255.18 (4092.02–6493.68)
BBFS2	4	13 (12/1)	16:27	8-May-19	1.35 (1.13–3.04)	7.725	7.725	30.21 (28.84–30.81)	2158.29 (854.84–3064.49)
BBFS3	3	33 (32/1)	16:53	10-May-19	3.41 (3.04–4.08)	7.65	7.65	29.10 (28.18–30.05)	2916.84 (1522.82–3489.36)
BBFS4	3	5 (5/0)	18:35	13-Sep-19	2.44 (1.59–4.08)	12.5	12.5	29.99 (28.74–30.70)	5060.22 (4126.10–5829.99)
BBFS5	3	7 (6/1)	19:46	14-Sep-19	3.36 (1.71–4.77)	9.9	9.9	30.79 (29.82–31.42)	3562.787 (1923.178–4804.21)
BBFS1*	3	4 (3/1)	19:12	24-Sep-19	1.53 (0.33–2.47)	17.15	17.15	29.38 (28.-64–29.68)	5443.14 (3661.82–6485.72)
MML1	2	2 (1/1)	8:55	25-Feb-15	3.50 (2.92–4.08)	2.13	2.2	28.20 (27.6–28.8)	418.10 (290.61–545.58)
MML2	2	2 (0/2)	8:45	26-Feb-15	3.94 (3.67–4.22)	2.26	2.2	29.40 (29.2–29.6)	386.33 (355.26–417.40)
MML3	2	2 (0/2)	9:10	27-Feb-15	3.75 (3.00–4.50)	1.98	1.8	29.65 (29.5–29.8)	353.14 (344.17–362.117)
MML4	2	1 (0/1)	9:10	2-Mar-15	3.46 (3.00–3.92)	3.07	3	29.30	519.94
MML5	2	2 (0/2)	9:00	3-Mar-15	3.83 (3.00–4.67)	2.69	2.6	29.45 (29.1–29.8)	453.40 (391.09–515.72)
MML6	2	3 (0/3)	8:55	4-Mar-15	4.12 (2.67–5.58)	2.4	2.6	29.13 (29.0–29.3)	441.31 (390.70–489.75)
MML7	2	5 (0/5)	9:05	6-Mar-15	4.54 (3.67–5.42)	2.06	2.2	29.12 (28.7–29.6)	361.99 (290.61–424.35)
MML8	1	5 (0/5)	8:32	20-Jan-16	7.63	2.05	2.2	29.46 (29.0–29.9)	341.56 (250.05–401.19)
MML9	1	2 (0/2)	8:32	21-Jan-16	6.30	1.74	1.8	29.60 (29.6–29.6)	288.65 (281.25–296.05)
MML10	1	5 (5/0)	8:33	6-Feb-16	6.37	2.04	2.2	30.42 (30.2–30.7)	519.18 (468.57–602.65)
MML11	1	1 (1/0)	8:50	17-Feb-16	5.92	2.52	2.6	30.30	645.70
MML12	2	11 (11/0)	9:32	4-Feb-16	4.15 (4.00–4.30)	2.95	3	29.25 (29.2–29.4)	690.87 (511.45–881.68)
MML13	1	2 (0/2)	8:45	19-Jan-16	7.33	1.9	3	29.35 (29.1–29.6)	394.77 (375.07–414.47)
MML14	1	3 (0/3)	9:00	18-Jan-16	8.42	2.1	2.2	29.87 (29.7–30.0)	354.61 (336.78–386.87)
MML15	1	6 (6/0)	9:02	2-Feb-16	8.55	2.11	2.2	30 (29.8–30.3)	493.22 (408.14–542.17)
MML16	1	5 (0/5)	9:05	16-Feb-16	8.83	2.27	2.2	29.80 (29.6–30.0)	327.52 (286.57–380.71)

Mean values are presented with the range of observed values in parentheses. Temperature and $\dot{M}_{O_2whole}$ are representative of values observed only during calibration intervals, while all other values are representative of all observed data throughout all trials.

*Individual BBFS1 was used twice for trials because it was opportunistically captured during two separate sampling seasons. Because the mass of BBFS1 was substantially different between these seasons, it was treated as two individuals for modelling purposes.

Journal of Experimental Biology (2021) 224, jeb233544. doi:10.1242/jeb.233544

Journal of Experimental Biology (2021) 224, jeb233544. doi:10.1242/jeb.233544

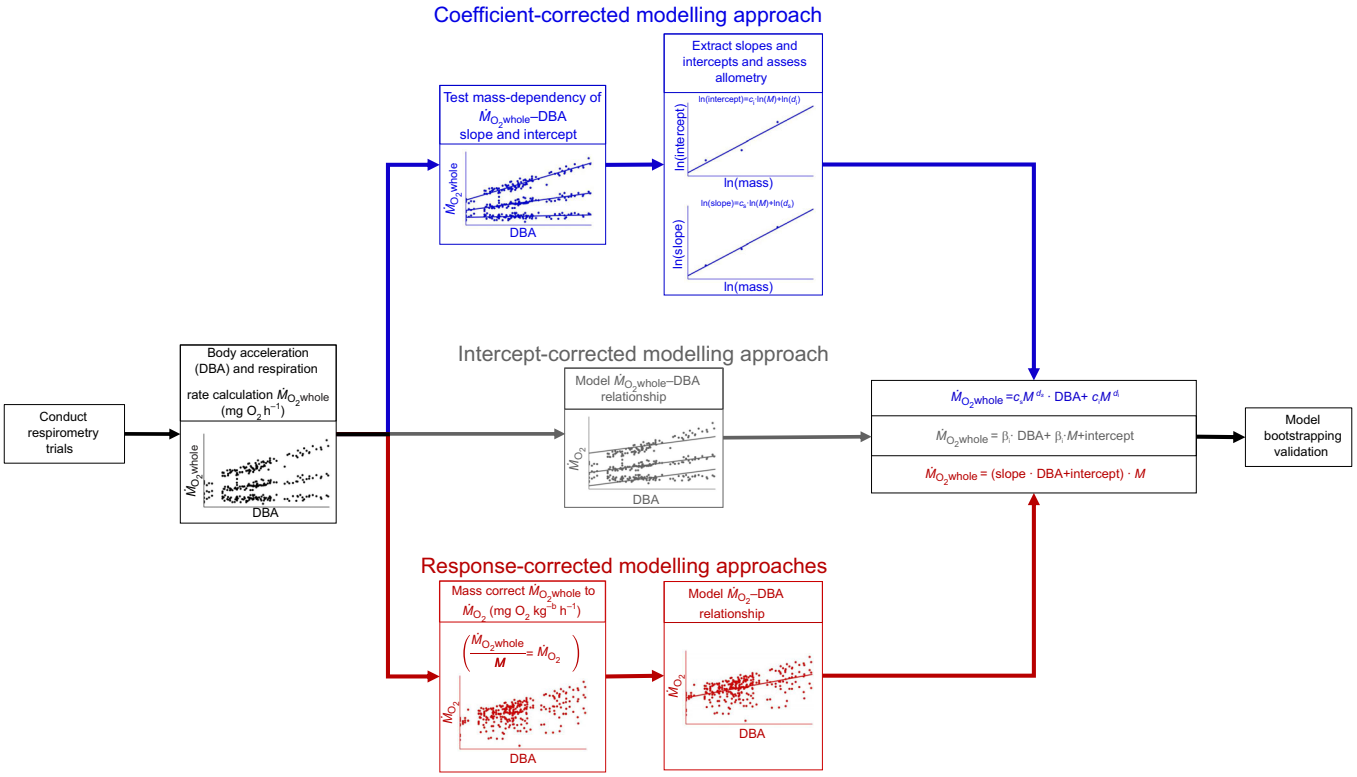

Fig. 1. Workflow of establishing $\dot{M}_{O_2}$ predictive models from respirometry and body acceleration data. All steps from initial data collection through final model validation are shown for the coefficient-corrected approach (top), intercept-corrected approach (middle) and response-corrected approaches (bottom). Mass corrections in response-corrected approaches can be either isometric ($\dot{M}_{O_2}$whole divided by M^1) or allometric ($\dot{M}_{O_2}$whole divided by M^b), where b is a species-specific scaling rate and M is mass (kg). Plots are provided for clarity but do not display real data.

Second, the effects of mass on the intercept (β_i) and slope (β_s) of these regressions were examined, under the assumption that the intercept and slope scale allometrically according to a power function, similar to Eqn 1. Given that logarithmic linear functions are the linear equivalent of power functions, we examined the effect of mass on the intercept and slope of regressions using general linear models, following the form of natural logarithmic functions:

$$\ln(\beta_i) = \ln(c_i) + d_i \cdot \ln(M), \quad (6)$$

$$\ln(\beta_s) = \ln(c_s) + d_s \cdot \ln(M), \quad (7)$$

where M is the mass (kg), c_i and d_i are, respectively, the intercept and slope of the natural logarithm function describing the effect of mass on β_i, and c_s and d_s are, respectively, the intercept and slope of the natural logarithm function describing the effect of mass on β_s (Fig. 1). For this analysis, a separate β_i and β_s were extracted from the linear mixed-effects model (Eqn 5) for each mass class, and used to estimate c_i, d_i, c_s and d_s. To compare the effect of mass on β_i and β_s, we estimated 95% confidence intervals for d_i and d_s using the 'confint' function in R. If confidence intervals did not overlap, the effects of mass on d_i and d_s were considered to be statistically different (Schenker and Gentleman, 2001).

To establish a single $\dot{M}_{O_2\text{whole}}$ predictive equation that could be applied across all mass classes, these natural logarithm functions were then exponentiated to allometric power functions:

$$\beta_i = c_i M^{d_i}, \quad (8)$$

$$\beta_s = c_s M^{d_s}, \quad (9)$$

describing the effect of mass on the $\dot{M}_{O_2\text{whole}}$–VeDBA regression intercept (Eqn 8) and slope (Eqn 9). Eqns 8 and 9 were then substituted into Eqn 4, yielding a final predictive equation:

$$\dot{M}_{O_2\text{whole}} = c_i M^{d_i} + c_s M^{d_s}(\text{VeDBA}). \quad (10)$$

As this equation incorporates mass effects into both the intercept and slope regression coefficients, it will hereafter be referred to as the 'coefficient-corrected approach'.

Other modelling approaches

To compare the accuracy of the coefficient-corrected approach, with other approaches used throughout the literature, we fit additional predictive equations based on methods commonly used throughout literature (see 'Response-corrected approach' and 'Intercept-corrected approach' subsections below). As previously mentioned, two other modelling approaches have been used to incorporate mass effects into $\dot{M}_{O_2}$ predictive equations. The more commonly applied approach uses mass-specific $\dot{M}_{O_2}$ (mg O_2 kg^{-b} h^{-1}) when modelling the $\dot{M}_{O_2}$–DBA relationship, rather than modelling $\dot{M}_{O_2\text{whole}}$ (mg O_2 h^{-1}) (e.g. Enstipp et al., 2011; Lear et al., 2017). By using mass-specific $\dot{M}_{O_2}$, these methods incorporate mass effects into the response variable of predictive equations, as opposed to directly incorporating mass effects into the coefficients of predictive models. Accordingly, this approach will henceforth be referred to as 'response-corrected approach'. The second modelling approach directly models $\dot{M}_{O_2\text{whole}}$ as a function of body mass by including mass as a covariate within model formulations. However, unlike the coefficient-corrected approach here, previous applications have not considered interactive effects between mass and other covariates (e.g. Brownscombe et al., 2017), and therefore only incorporated an effect of mass on the intercept of the $\dot{M}_{O_2}$–DBA regression. Accordingly,

this approach will henceforth be referred to as the 'intercept-corrected approach'.

Response-corrected approach

Two models were fitted using the response-corrected approach. For the first model, $\dot{M}_{O_2whole}$ estimates were isometrically corrected by dividing $\dot{M}_{O_2whole}$ by animal mass in kg (M), resulting in mass-specific $\dot{M}_{O_2}$ in mg O_2 kg^{-1} h^{-1}. For the second model, $\dot{M}_{O_2whole}$ estimates were allometrically corrected by dividing $\dot{M}_{O_2whole}$ by animal mass in kg raised to an allometric BMR scaling exponent (M^b), resulting in mass-specific $\dot{M}_{O_2}$ in mg O_2 kg^{-b} h^{-1}. For this study, an allometric exponent of 0.86 was used, a value widely regarded as the universal elasmobranch SMR mass-scaling exponent (Sims, 2000). Models were fitted using the glm function in R, assuming a Gaussian error structure, with mass class included as a continuous covariate. Mass was not considered as a categorical variable for these models, as these methods are based on the most common modelling approaches used in calibrations of DBA data for predicting FMR of animals and were used for comparison with the coefficient-corrected approach. These two response-corrected models will hereafter be referred to as the 'isometric response-corrected model' and the 'allometric response-corrected model'.

To allow comparison with models that estimate $\dot{M}_{O_2whole}$, mass-specific estimates from the isometric response-corrected model and allometric response-corrected model were corrected *post hoc* to $\dot{M}_{O_2whole}$ by multiplying estimates by M and $M^{0.86}$, respectively.

Intercept-corrected approach

A single model was fitted using the intercept-corrected approach. To do so, we used a linear mixed-effects model (lme4 package), which included VeDBA and mass class as continuous covariates to explain variation in $\dot{M}_{O_2whole}$. It is important to note that treating mass as a continuous covariate assumes mass has an isometric effect on the intercept of the modelling relationship, which may not accurately represent the species' specific BMR allometric scaling rate. Therefore, treating mass class as a categorical variable may produce a more accurate estimation of $\dot{M}_{O_2whole}$. However, treatment of mass as a categorical variable was not considered here because this approach was strictly based on the approaches of previous calibration studies and was used only for comparison with the coefficient-corrected approach.

Model validation and error comparison

We used a bootstrap validation technique to estimate prediction error of each modelling approach. In this technique, we bootstrapped 1000 datasets of VeDBA and $\dot{M}_{O_2whole}$ observations (n=124 per dataset) from all available respirometry data, and fitted new predictive models for each data set. A coefficient-corrected model, an isometric response-corrected model, an allometric response-corrected model and an intercept-corrected model were fitted to each bootstrapped dataset, as per the modelling processes above, and each model was used to predict $\dot{M}_{O_2whole}$ for each observation of VeDBA in the corresponding dataset. The root mean square (RMS):

$$\mathrm{RMS} = \sqrt{\frac{\sum \left(\dot{M}_{O_2whole,observed} - \dot{M}_{O_2whole,predicted}\right)^2}{N_{obs}}}, \quad (11)$$

and coefficient of variation (COV):

$$\mathrm{COV} = \frac{\mathrm{RMS} \times 100}{\dot{M}_{O_2whole,observed}}, \quad (12)$$

were calculated for each bootstrapped model and averaged across all 1000 bootstrapped models to estimate the prediction error of each modelling approach. In Eqns 11 and 12, $\dot{M}_{O_2whole,observed}$ and $\dot{M}_{O_2whole,predicted}$ are the observed and predicted $\dot{M}_{O_2whole}$ values, and N_{obs} is the number of observations. In addition, the marginal R^2 was extracted from each bootstrapped model and the overall mean was used as another quantification of model performance.

To assess prediction error in more detail, we examined how prediction error changed as a function of body mass and activity level by repeatedly simulating a day in the life of 100 sharks per mass class, similar to Green et al. (2009). A sample size of 100 sharks per mass class was used to reduce likelihood of type II errors. In these simulations, bootstrapping was used to simulate an observation every 15 min over a 24-h period for each shark, resulting in 96 observations per shark. Respirometry data were split into two resampling pools, separating inactive (intervals where sharks rested) and active (i.e. intervals where sharks swam) data. Simulated observations were drawn at random with replacement (i.e. bootstrapped) from these resampling data pools. Inactive simulated observations were created by bootstrapping from the inactive data pool, whereas active simulated observations were created by bootstrapping from the active data pool. $\dot{M}_{O_2whole}$ was predicted for all simulated observations based on the predictive equations from each of the modelling approaches, and the mean RMS (Eqn 11) and mean COV (Eqn 12) of each model were calculated individually for all body mass classes. This process was repeated for each shark, varying the amount of time sharks spent active between 0 and 100%, increasing by one percentage point for each successive iteration. The 12.5 and 14.65 kg mass classes were excluded from the simulation, as inactive and active data were not both available to bootstrap simulated datasets for these classes (Table 1).

All statistical analysis was carried out in R v3.6.3 (https://www.r-project.org/).

RESULTS

Sample size

A total of 43 respirometry trials (mean±s.d.=1.95±0.88 per individual fish; mean duration=21.14±10.77 min; all means are presented ±s.d. unless otherwise indicated) were conducted on 21 individuals, ranging in body mass from 1.74 to 17.15 kg (mean=4.81±4.55 kg; Table 1). Once grouped by mass, a total of 10 individual mass classes were retained (Table 1). From these trials, 129 $\dot{M}_{O_2whole}$ estimations (mean per class=12.90±10.23) were obtained for calibrations. However, five $\dot{M}_{O_2whole}$ observations from Bimini sharks were deemed as biologically impossible because they were twice as high as other estimates with similar VeDBA. While it is unclear what caused such erroneous values, these may have been associated with short power outages, unnoticed by personnel, causing insufficient water flow over the DO probe. Nonetheless, these observations were removed from analysis, leaving 124 observations (mean per class=12.40±10.21), including 37 inactive (mean per class=3.70±5.85) and 87 active observations (mean per class=8.70 ±8.66) (Table 1). From these 124 observations, $\dot{M}_{O_2whole}$ ranged from 286.57 to 6493.68 mg O_2 h^{-1} (Table 1). After correction for acceleration sensor noise (0.018***g***; representing a mean 14.7% of active interval VeDBA), VeDBA ranged from −0.014 to 0.172***g*** (Fig. 3). Water temperature during calibration intervals ranged from 27.32 to 31.42°C (mean=29.52±0.81°C) (Table 1).

Coefficient-corrected model

There was a strong positive correlation between VeDBA and $\dot{M}_{O_2whole}$, with both the slope and intercept displaying significant

Journal of Experimental Biology (2021) 224, jeb233544. doi:10.1242/jeb.233544

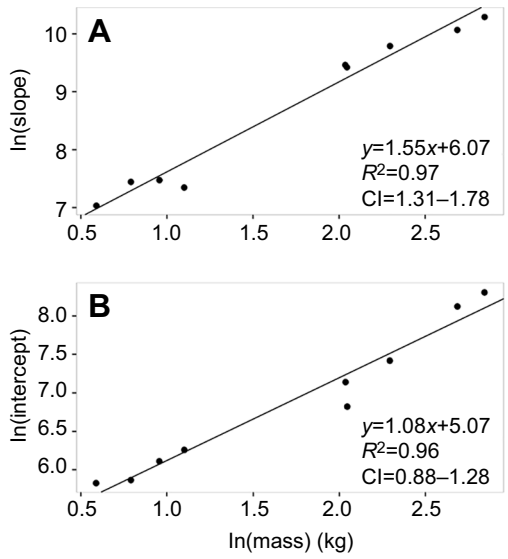

Fig. 2. Body mass scaling of the slope and intercept of the $\dot{M}_{O_2whole}$–VeDBA relationship. (A) Slope and (B) intercept values were extracted from the coefficient-corrected linear mixed-effects model, natural log transformed, and regressed against the natural log of body mass. Linear regression equations (slope regression: t=15.7, P<0.01; intercept regression: t=12.60, P<0.01) and associated correlation coefficient (R^2) and slope confidence intervals (CI) are displayed for each scaling relationship.

allometry (Fig. 3). The final linear model included VeDBA and an effect of mass class on both the slope and intercept terms (Table 2). From this model, a total of nine slopes and intercepts were estimated, which were used to assess the allometry of the $\dot{M}_{O_2whole}$–VeDBA relationship. The 12.5 kg mass class was excluded from this scaling assessment because all $\dot{M}_{O_2}$ observations for this class occurred over a small range of DBA values, which resulted in a negative linear relationship (Fig. S1). The intercept of the $\dot{M}_{O_2whole}$–VeDBA regressions increased with an allometric exponent of 1.08 (CI=0.88–1.28, t=12.60, P<0.01, R^2=0.96; Fig. 2B), whereas the slope increased at a significantly steeper rate of 1.55 (CI=1.31–1.78, t=15.71, P<0.01, R^2=0.97; Fig. 2A), yielding a final predictive equation of:

$$\dot{M}_{O_2whole} = (154.51 \cdot M^{1.08}) + ((433.87 \cdot M^{1.55}) \cdot \text{VeDBA}), \quad (13)$$

where M is individual wet body mass in kg.

The final predictive model explained 97.91% of the variance (marginal R^2) in $\dot{M}_{O_2whole}$. Overall, the model tended to overestimate $\dot{M}_{O_2whole}$, with a mean error (COV) of 19.54% (RMS=329.99 mg O_2 h^{-1}). When only considering active data, the model had lower error (COV=17.07%, RMS=376.41 mg O_2 h^{-1}) than when only considering inactive data (COV=31.65%, RMS=78.34 mg O_2 h^{-1}).

Response-corrected models

VeDBA had a significant influence on both isometrically corrected mass-specific $\dot{M}_{O_2}$ (t=16.01, P<0.001, R^2=0.68) and allometrically corrected mass-specific $\dot{M}_{O_2}$ (t=13.81, P<0.001, R^2=0.61). The resulting predictive equations were:

$$\dot{M}_{O_2} = 169.73 + (1441.37 \cdot \text{VeDBA}), \quad (14)$$

for the isometric response-corrected model and:

$$\dot{M}_{O_2} = 197.01 + (2115.54 \cdot \text{VeDBA}), \quad (15)$$

for the allometric response-corrected model. The isometric response-corrected model had a mean error of 24.23% (RMS=589.78 mg O_2 h^{-1}), whereas the allometric response-corrected model had a mean error of 31.77% (RMS=589.78 mg O_2 h^{-1}).

Intercept-corrected model

VeDBA (t=15.345, P<0.001) and mass (t=15.345, P<0.001) had significant positive influences on $\dot{M}_{O_2whole}$ and explained 81.11% of variance (marginal R^2). The resulting predictive equation was:

$$\dot{M}_{O_2} = -636.83 + (5669.43 \cdot \text{VeDBA}) + (357.97 \cdot M), \quad (16)$$

where M is individual body mass in kg. Overall, the intercept-corrected model had a mean error of 22.47% (RMS=461.89 mg O_2 h^{-1}). Notably, the model tended to have substantially greater error for lower activity levels than higher activity levels across all body sizes (Fig. 3). When only considering active data, the model had lower error (COV=16.67%, RMS=461.11 mg O_2 h^{-1}) than when only considering inactive data (COV=85.12%, RMS=464.33 mg O_2 h^{-1}).

Model error comparison

All models predicted similar $\dot{M}_{O_2whole}$ for individuals near the midrange of masses; however, there was greater variation in model estimates for the larger and smaller masses (Fig. 4). For sharks smaller than 7.65 kg, the intercept-corrected model produced the lowest $\dot{M}_{O_2whole}$ estimates at lower activity levels; however, this shifted as activity level increased, with the coefficient-corrected model producing the lowest estimates when animals were active more than 35% of the time. In contrast, for sharks larger than 7.65 kg, the intercept-corrected model produced the highest $\dot{M}_{O_2whole}$ estimates across all activity levels and the allometric response-corrected model produced the lowest $\dot{M}_{O_2whole}$ estimates (Fig. 4, Fig. S2).

Overall, the coefficient-corrected model consistently had the lowest error across all body sizes and activity levels. The models with the highest error varied by body mass, with the intercept-corrected model generally having the highest error for smaller body sizes and the allometric response-corrected model having the highest error for larger body sizes (Fig. 4). The simulation revealed systematic mass biases in the isometric response-corrected model, the allometric response-corrected model and the intercept-corrected model. Estimation error of the response-corrected models tended to increase with increased body mass. In contrast, estimation error of the intercept-corrected model tended to decrease with body mass (Fig. 4, Fig. S2). However, no mass-associated bias was present in the estimates of the coefficient-corrected model (Fig. 4, Fig. S2). Differences in COV between models were smallest for the middle mass classes but varied more widely between models as a function of activity at the lower and higher masses (Fig. 4). At lower masses, the difference between model COV increased with increased time spent active, whereas the difference between model COV at larger masses was relatively consistent (Fig. 4). Overall, model COV tended to decrease with increased time spent active, particularly in the coefficient-corrected model (Fig. 4).

DISCUSSION

Despite the prominent influence that body size exerts on many aspects of animal biomechanics and physiology, no study has assessed the allometric dependence of the relationship between $\dot{M}_{O_2}$ and DBA and its effect on the accuracy of $\dot{M}_{O_2}$ predictive equations. By individually assessing the scaling of the $\dot{M}_{O_2whole}$–VeDBA slope and intercept, we validated that DBA per unit metabolism is scale dependent, and this dependency varies from that of BMR. As such, we found that directly accounting for

Journal of Experimental Biology (2021) 224, jeb233544. doi:10.1242/jeb.233544

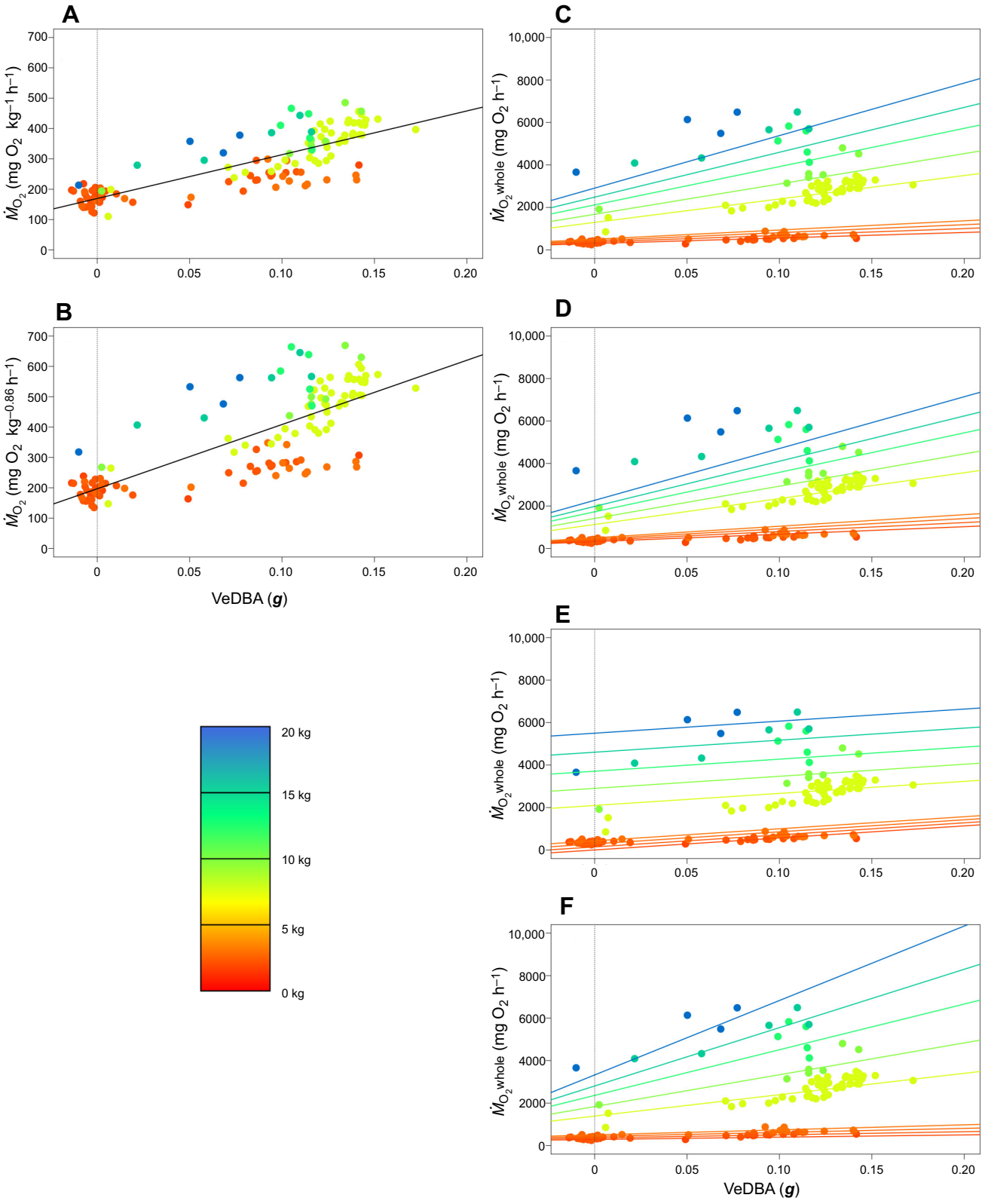

Fig. 3. Model predictions overlaid on observed data from respirometry calibration trials. The isometric response-corrected model (A) and allometric response-corrected model (B) were fitted to mass-specific $\dot{M}_{O_2}$ values, whereas the intercept-corrected model (E) and coefficient-corrected model (F) were fitted to $\dot{M}_{O_2whole}$ values (n=127). For comparison between models, isometric and allometric fits were corrected to $\dot{M}_{O_2whole}$ by multiplying estimates by a factor of M^1 (C) and $M^{0.86}$ (D), respectively, where M represents mass (kg). Observations and linear model fits are colour coded according to mass class. Vertical dotted lines represent the point of no activity, indicating the intercept of linear estimators.

Journal of Experimental Biology (2021) 224, jeb233544. doi:10.1242/jeb.233544

Table 2. Model selection table for the coefficient-corrected linear mixed-effects model

Model	Covariates	d.f.	logLik	AIC	ΔAIC
1	VeDBA×Mass+Mass	21	−847.2	1736.5	0
2	VeDBA+Mass	12	−908.3	1840.5	104.07
3	Mass	11	−932.3	1886.6	150.1
4	VeDBA	3	−1075	2156.9	420.43
5	Intercept	2	−1097	2198.5	462.02

This model was for the first stage of the modelling approach, used to explore the relationship between $\dot{M}_{O_2whole}$ and VeDBA. × indicates an interaction between terms. Models are ranked based on Akaike's information criterion (AIC) values. Degrees of freedom (d.f.) and log-likelihood (logLik) are shown for each model.

different body-mass scaling effects within model slope and intercept coefficients produces substantially more accurate estimates of oxygen consumption rates than other commonly applied modelling approaches. While all models performed similarly for individuals near the mean mass of calibrated animals, more commonly applied intercept-corrected and response-corrected approaches appeared to have substantial mass- and activity-associated biases that were not present within the coefficient-corrected approach. As a result, the coefficient-corrected approach consistently had the lowest prediction error across all body sizes (Fig. 4). Additionally, as activity levels of animals increased, the disparity in estimation error between the coefficient-corrected and response-corrected models tended to increase, whereas the disparity in estimation error between coefficient-corrected and intercept-corrected models tended to decrease. However, the covariate-corrected approach demonstrated the smallest activity bias, and again outperformed other modelling approaches across activity levels.

The differences in estimation error between modelling approaches could have large implications when calibrated predictive equations are applied to predict energy expenditure of animals in the wild. For example, for a 17.15 kg lemon shark that is active 50% of the time, the difference between the daily energy expenditure estimated by the isometric response-corrected model and coefficient-corrected model would be 17,114.83 mg O_2 day^{-1}. This difference converts to 232.591 kJ day^{-1} (Jobling, 1995), approximately one yellow fin mojarra (*Gerres cinereus*), the primary prey of juvenile lemon sharks in Bimini (Pettitt-Wade et al., 2011), or a 25% increase in the daily energetic requirements. This difference would be proportionally even larger for smaller body sizes, where the disparity between model estimation error was greater. As a result, with such improvements over other modelling approaches for incorporating mass effects into $\dot{M}_{O_2}$ estimations, we strongly recommend the coefficient-corrected approach for establishing $\dot{M}_{O_2}$ predictive equations across different body sizes.

Although the coefficient-corrected approach provided more robust estimates of energy expenditure than currently used approaches, several opportunities for improvement remain. Foremost, although conducted *pre hoc* in this study, an ideal full model should incorporate a temperature correction factor in the intercept term. Additionally, more balanced sampling across activity levels and mass classes would allow for a mechanistic examination of error accumulation, which may help to identify and incorporate further correction factors into models. Of course, conducting respirometry experiments over a range of body sizes presents logistical and ethical complexities that may limit sample size, as was the case in this study. However, in respirometers with small system to animal volume ratios, which facilitate rapid respiration measurement response times (Clark et al., 2013), calibration interval durations could be decreased to facilitate larger sample sizes per trial. Additionally, when ethically viable, animals could be left in the respirometer for longer acclimation periods or more trials, potentially facilitating greater variability in behaviours as animals become more comfortable with the system. While more calibration intervals within trials may also increase variability of sampled activity levels, using forced activity protocols (e.g. swim tunnels or treadmills) may ensure that observations are obtained across all activity levels, although it is

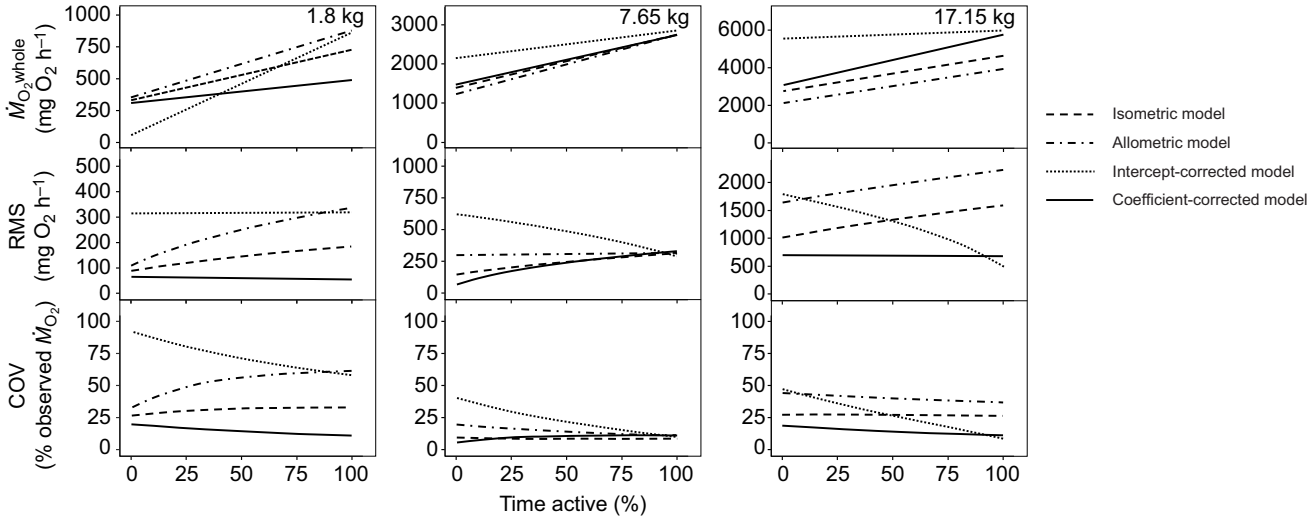

Fig. 4. Simulation showing the effect of different modelling techniques when accounting for body mass in $\dot{M}_{O_2whole}$ estimations across a range of activity levels. A day in the life of 100 sharks for each mass class (n=8) was repeatedly simulated, where the percentage of time spent active was varied. For clarity, only the 1.8 kg (left), 7.65 kg (middle column) and 17.15 kg (right) mass classes are shown. Whole-animal oxygen consumption rate ($\dot{M}_{O_2whole}$; top), root mean square (RMS; middle row) and coefficient of variation (COV; bottom) were calculated over the full range of activity for each body mass using the isometric response-corrected (dashed line), allometric response-corrected (dot-dashed line), intercept-corrected (dotted) and coefficient-corrected (solid line) approaches. Note that the $\dot{M}_{O_2whole}$ and RMS scales vary between mass classes for clarity of differences between models.

of note that such protocols may introduce other bias through alteration of natural gaits in many species (Lear et al., 2019; Whitney et al., 2018).

As the mechanics and external forces defining the $\dot{M}_{O_2}$–DBA relationship depend on numerous factors such as body form (Alexander, 2005; Bale et al., 2014), locomotory type (Alexander, 2005; Schmidt-Nielsen, 1972) and viscosity of the environmental medium (Schmidt-Nielsen, 1972; Wieser and Kaufmann, 1998), $\dot{M}_{O_2}$–DBA slope and intercept scaling exponents will inevitably vary between taxa. However, when corrected for body mass, the $\dot{M}_{O_2}$–DBA relationship may be similar across geometrically similar species, potentially allowing for common equations to be established for estimating energy expenditure from DBA (Gleiss et al., 2011). In fact, Halsey et al. (2009) and Miwa et al. (2015) both established common predictive equations for estimating the energy expenditure across a range of species, although the accuracy of estimations using these interspecifically derived equations was not assessed. Nonetheless, the establishment of common $\dot{M}_{O_2}$ predictive equations suggests that fundamental laws of biomechanics and physics may constrain the ratio of the $\dot{M}_{O_2}$–DBA slope to intercept scaling exponents to universal values. Further calibration experiments conducted with various taxa will determine the scatter in intraspecific scaling exponents and may help to identify such biomechanical and physical laws governing the $\dot{M}_{O_2}$–DBA relationship.

In circumstances in which respiration measurements cannot be acquired from a range of body masses (e.g. facility or animal availability limitations), and thus response-corrected models or intercept-corrected models must be extrapolated, the biases of such models must be carefully considered. Foremost, bias drastically increased with increasing difference in body mass between the median mass of individuals in the calibration experiments and individuals for which respiration rate was being estimated. Thus, to minimize estimation error, caution must be exercised when extrapolating equations to animals with substantially different body masses than those used in calibration experiments. Additionally, models demonstrated large activity bias, where the estimation error drastically changed as a function of increased activity, particularly for smaller body masses. However, the direction of the bias was opposite between models, where estimation error of the intercept-corrected model decreased with increased activity and estimation error of response-corrected models tended to increase with activity. This activity bias may partially be a product of the relatively larger spread of $\dot{M}_{O_2}$ and VeDBA measurements during active calibration intervals compared with inactive intervals. Using forced activity protocols to ensure more balanced sampling of different activity levels throughout calibration experiments would help to elucidate the source of this error. Nevertheless, this activity level associated bias indicates that as animals become more active, *post hoc* corrections based on isometric or allometric BMR scaling rates introduce increased error. In contrast, estimation error of the intercept-corrected model decreased as animals became more active, and estimates for larger body sizes had similar error as the coefficient-corrected approach at particularly high (>75%) activity levels. However, the rapid and nonlinear decrease in estimation error with increased activity could result in large and unpredictable variation in estimates with small changes in activity. Thus, it is imperative to independently account for separate scaling rates of the $\dot{M}_{O_2}$–DBA slope and intercept when estimating respiration of highly active species, especially for smaller body sizes, where a small change in activity may represent a relatively larger change in overall energy requirements.

We found that isometric mass-specific corrections produced more accurate estimates than using a universal allometric correction of $M^{0.86}$. However, the higher performance of the isometric correction was likely a product of the BMR scaling rate of lemon sharks in this study being closer to isometry. In species with lower BMR scaling exponents, such as mammals (White and Seymour, 2003), it is likely that a lower nonproportional allometric mass-correction would perform better. However, the intercept-corrected model, which included an isometric effect on the intercept only, outperformed the allometric response-corrected model at lower body sizes, indicating that additional factors led to the greater performance of the isometric response-corrected model. The higher performance of the isometric correction, alternatively, may also be due to the observed scaling rate of the $\dot{M}_{O_2}$–DBA slope falling closer to the isometric exponent than the universal BMR allometric exponent. Nevertheless, the coefficient-corrected approach circumnavigates such issues by separately identifying slope and intercept scaling rates and outperforms commonly applied response-corrected and intercept-corrected modelling approaches. Given that we confirmed that DBA per unit oxygen (i.e. regression slope) scales allometrically at a different rate to that of BMR, where possible it is essential to use the coefficient-corrected approach when establishing $\dot{M}_{O_2}$–DBA predictive models.

Acknowledgements
We thank Bimini Biological Field Station staff, including C. White, V. Heim, C. Mason, S. Hart, E. Richardson, H. Lintott, D. Warburton, W. Nambu, A. Warrior, K. Yang and J. Whicheloe, as well as L. Harlow and numerous other interns who were essential for capturing sharks and conducting field trials in Bimini. Mote Marine Laboratory staff, including J. Morris, A. Ontkos, A. Osowski, A. Andres and R. Hueter, and numerous interns were essential to captive maintenance of sharks and respirometry experiments at MML. Additionally, we thank R. Daly, S. H. Gruber and T. L. Guttridge for providing logistical support.

Competing interests
The authors declare no competing or financial interests.

Author contributions
Conceptualization: E.B., A.C.G.; Methodology: E.B., K.O.L., L.R.B., N.M.W., N.J.A., A.C.G.; Validation: E.B.; Formal analysis: E.B.; Investigation: E.B.; Data curation: E.B., K.O.L., L.R.B.; Writing - original draft: E.B.; Writing - review & editing: E.B., K.O.L., L.R.B., N.M.W., M.J.S., N.J.A., A.C.G.; Visualization: E.B.; Supervision: N.J.A., A.C.G.; Project administration: N.M.W., M.J.S., A.C.G.; Funding acquisition: E.B., N.M.W., A.C.G.

Funding
Research was generously supported by grants from Save Our Seas Foundation (project no. 402) to E.E.B. and A.C.G. and the National Science Foundation (OCE no. 1156141) to N.M.W., A.C.G. and R. E. Hueter. E.E.B. was supported by an Australian Government Research Training Program Scholarship throughout this study.

Data availability
Data are available from the figshare digital repository: https://figshare.com/articles/dataset/JEB_lemon_respirometry_data_csv/14176994

Supplementary information
Supplementary information available online at https://jeb.biologists.org/lookup/doi/10.1242/jeb.233544.supplemental

References
Alexander, R. M. (2005). Models and the scaling of energy costs for locomotion. *J. Exp. Biol.* **208**, 1645-1652. doi:10.1242/jeb.01484

Baldridge, H. D., Jr. (1970). Sinking factors and average densities of Florida sharks as functions of liver buoyancy. *Copeia* **1970**, 744-754. doi:10.2307/1442317

Bale, R., Hao, M., Bhalla, A. P. S. and Patankar, N. A. (2014). Energy efficiency and allometry of movement of swimming and flying animals. *Proc. Natl Acad. Sci. USA* **111**, 7517-7521. doi:10.1073/pnas.1310544111

Bishop, C. M. (1999). The maximum oxygen consumption and aerobic scope of birds and mammals: getting to the heart of the matter. *Proc. R. Soc. Lond. B Biol. Sci.* **266**, 2275-2281. doi:10.1098/rspb.1999.0919

Bouyoucos, I. A., Montgomery, D. W., Brownscombe, J. W., Cooke, S. J., Suski, C. D., Mandelman, J. W. and Brooks, E. J. (2017). Swimming speeds and metabolic rates of semi-captive juvenile lemon sharks (*Negaprion brevirostris*, Poey) estimated with acceleration biologgers. *J. Exp. Mar. Biol. Ecol.* **486**, 245-254. doi:10.1016/j.jembe.2016.10.019

Brownscombe, J. W., Cooke, S. J. and Danylchuk, A. J. (2017). Spatiotemporal drivers of energy expenditure in a coastal marine fish. *Oecologia* **183**, 689-699. doi:10.1007/s00442-016-3800-5

Brownscombe, J. W., Lennox, R. J., Danylchuk, A. J. and Cooke, S. J. (2018). Estimating fish swimming metrics and metabolic rates with accelerometers: the influence of sampling frequency. *J. Fish Biol.* **93**, 207-214. doi:10.1111/jfb.13652

Butler, P. J., Green, J. A., Boyd, I. L. and Speakman, J. R. (2004). Measuring metabolic rate in the field: the pros and cons of the doubly labelled water and heart rate methods. *Funct. Ecol.* **18**, 168-183. doi:10.1111/j.0269-8463.2004.00821.x

Byrnes, E. E., Lear, K. O., Morgan, D. L. and Gleiss, A. C. (2020). Respirometer in a box: development and use of a portable field respirometer for estimating oxygen consumption of large-bodied fishes. *J. Fish Biol.* **96**, 1045-1050. doi:10.1111/jfb.14287

Clark, T. D., Sandblom, E. and Jutfelt, F. (2013). Aerobic scope measurements of fishes in an era of climate change: respirometry, relevance and recommendations. *J. Exp. Biol.* **216**, 2771-2782. doi:10.1242/jeb.084251

Clarke, A. and Johnston, N. M. (1999). Scaling of metabolic rate with body mass and temperature in teleost fish. *J. Anim. Ecol.* **68**, 893-905. doi:10.1046/j.1365-2656.1999.00337.x

da Silva, J. K. L., Garcia, G. J. M. and Barbosa, L. A. (2006). Allometric scaling laws of metabolism. *Phys. Life Rev.* **3**, 229-261. doi:10.1016/j.plrev.2006.08.001

Enstipp, M. R., Ciccione, S., Gineste, B., Milbergue, M., Ballorain, K., Ropert-Coudert, Y., Kato, A., Plot, V. and Georges, J.-Y. (2011). Energy expenditure of freely swimming adult green turtles (*Chelonia mydas*) and its link with body acceleration. *J. Exp. Biol.* **214**, 4010-4020. doi:10.1242/jeb.062943

Gillooly, J. F., Brown, J. H., West, G. B., Savage, V. M. and Charnov, E. L. (2001). Effects of size and temperature on metabolic rate. *Science* **293**, 2248-2251. doi:10.1126/science.1061967

Gleiss, A. C., Dale, J. J., Holland, K. N. and Wilson, R. P. (2010). Accelerating estimates of activity-specific metabolic rate in fishes: testing the applicability of acceleration data-loggers. *J. Exp. Mar. Biol. Ecol.* **385**, 85-91. doi:10.1016/j.jembe.2010.01.012

Gleiss, A. C., Wilson, R. P. and Shepard, E. L. C. (2011). Making overall dynamic body acceleration work: on the theory of acceleration as a proxy for energy expenditure. *Methods Ecol. Evol.* **2**, 23-33. doi:10.1111/j.2041-210X.2010.00057.x

Green, J. A., Halsey, L. G., Wilson, R. P. and Frappell, P. B. (2009). Estimating energy expenditure of animals using the accelerometry technique: activity, inactivity and comparison with the heart-rate technique. *J. Exp. Biol.* **212**, 471-482. doi:10.1242/jeb.026377

Halsey, L. G., Shepard, E. L. C., Quintana, F., Laich, A. G., Green, J. A. and Wilson, R. P. (2009). The relationship between oxygen consumption and body acceleration in a range of species. *Comp. Biochem. Physiol. A Mol. Integr. Physiol.* **152**, 197-202. doi:10.1016/j.cbpa.2008.09.021

Jobling, M. (1995). Fish bioenergetics. *Oceanogr. Literature Rev.* **9**, 785.

Killen, S. S., Costa, I., Brown, J. A. and Gamperl, A. K. (2007). Little left in the tank: metabolic scaling in marine teleosts and its implications for aerobic scope. *Proc. R. Soc. B* **274**, 431-438. doi:10.1098/rspb.2006.3741

Kleiber, M. (1932). Body size and metabolism. *Hilgardia* **6**, 315-353. doi:10.3733/hilg.v06n11p315

Kozłowski, J., Konarzewski, M. and Gawelczyk, A. (2003). Cell size as a link between noncoding DNA and metabolic rate scaling. *Proc. Natl Acad. Sci. USA* **100**, 14080-14085. doi:10.1073/pnas.2334605100

Lear, K. O., Whitney, N. M., Brewster, L. R., Morris, J. J., Hueter, R. E. and Gleiss, A. C. (2017). Correlations of metabolic rate and body acceleration in three species of coastal sharks under contrasting temperature regimes. *J. Exp. Biol.* **220**, 397-407. doi:10.1242/jeb.146993

Lear, K. O., Whitney, N. M., Brewster, L. R. and Gleiss, A. C. (2019). Treading water: respirometer choice may hamper comparative studies of energetics in fishes. *Mar. Freshw. Res.* **70**, 437-448. doi:10.1071/MF18182

Lear, K. O., Morgan, D. L., Whitty, J. M., Whitney, N. M., Byrnes, E. E., Beatty, S. J. and Gleiss, A. C. (2020). Divergent field metabolic rates highlight the challenges of increasing temperatures and energy limitation in ectotherms. *Oecologia 193, 311-323*. doi:10.1007/s00442-020-04669-x

Lyons, G. N., Halsey, L. G., Pope, E. C., Eddington, J. D. and Houghton, J. D. R. (2013). Energy expenditure during activity in the American lobster *Homarus americanus*: correlations with body acceleration. *Comp. Biochem. Physiol. A Mol. Integr. Physiol.* **166**, 278-284. doi:10.1016/j.cbpa.2013.06.024

Miwa, M., Oishi, K., Nakagawa, Y., Maeno, H., Anzai, H., Kumagai, H., Okano, K., Tobioka, H. and Hirooka, H. (2015). Application of overall dynamic body acceleration as a proxy for estimating the energy expenditure of grazing farm animals: relationship with heart rate. *PLoS ONE* **10**, e0128042. doi:10.1371/journal.pone.0128042

Payne, N. L., Gillanders, B. M., Seymour, R. S., Webber, D. M., Snelling, E. P. and Semmens, J. M. (2011). Accelerometry estimates field metabolic rate in giant Australian cuttlefish *Sepia apama* during breeding. *J. Anim. Ecol.* **80**, 422-430. doi:10.1111/j.1365-2656.2010.01758.x

Pettitt-Wade, H., Newman, S. P., Parsons, K. T., Gruber, S. H. and Handy, R. D. (2011). Dietary metal and macro-nutrient intakes of juvenile lemon sharks determined from the nutritional composition of prey items. *Mar. Ecol. Prog. Ser.* **433**, 245-260. doi:10.3354/meps09114

Qasem, L., Cardew, A., Wilson, A., Griffiths, I., Halsey, L. G., Shepard, E. L. C., Gleiss, A. C. and Wilson, R. (2012). Tri-axial dynamic acceleration as a proxy for animal energy expenditure; should we be summing values or calculating the vector? *PLoS ONE* **7**, e31187. doi:10.1371/journal.pone.0031187

Robson, A. A., Halsey, L. G. and Chauvaud, L. (2016). Feet, heat and scallops: what is the cost of anthropogenic disturbance in bivalve aquaculture? *R. Soc. Open Sci.* **3**, 150679. doi:10.1098/rsos.150679

Sakamoto, K. Q., Sato, K., Ishizuka, M., Watanuki, Y., Takahashi, A., Daunt, F. and Wanless, S. (2009). Can ethograms be automatically generated using body acceleration data from free-ranging birds? *PLoS ONE* **4**, e5379. doi:10.1371/journal.pone.0005379

Schenker, N. and Gentleman, J. F. (2001). On judging the significance of differences by examining the overlap between confidence intervals. *Am. Stat.* **55**, 182-186. doi:10.1198/000313001317097960

Schmidt-Nielsen, K. (1972). Locomotion: energy cost of swimming, flying, and running. *Science* **177**, 222-228. doi:10.1126/science.177.4045.222

Sims, D. W. (2000). Can threshold foraging responses of basking sharks be used to estimate their metabolic rate? *Mar. Ecol. Prog. Ser.* **200**, 289-296. doi:10.3354/meps200289

Speakman, J. (1997). *Doubly Labelled Water: Theory and Practice*. Springer Science & Business Media.

Videler, J. J. (1993). *Fish Swimming*. Springer Science & Business Media.

Watanabe, Y. Y., Payne, N. L., Semmens, J. M., Fox, A. and Huveneers, C. (2019). Swimming strategies and energetics of endothermic white sharks during foraging. *J. Exp. Biol.* **222**, jeb185603. doi:10.1242/jeb.185603

West, G. B. and Brown, J. H. (2005). The origin of allometric scaling laws in biology from genomes to ecosystems: towards a quantitative unifying theory of biological structure and organization. *J. Exp. Biol.* **208**, 1575-1592. doi:10.1242/jeb.01589

West, G. B., Brown, J. H. and Enquist, B. J. (1997). A general model for the origin of allometric scaling laws in biology. *Science* **276**, 122-126. doi:10.1126/science.276.5309.122

White, C. R. and Seymour, R. S. (2003). Mammalian basal metabolic rate is proportional to body mass$^{2/3}$. *Proc. Natl Acad. Sci. USA* **100**, 4046-4049. doi:10.1073/pnas.0436428100

White, C. R., Cassey, P. and Blackburn, T. M. (2007). Allometric exponents do not support a universal metabolic allometry. *Ecology* **88**, 315-323. doi:10.1890/05-1883

Whitney, N. M., Pratt, H. L., Jr., Pratt, T. C. and Carrier, J. C. (2010). Identifying shark mating behaviour using three-dimensional acceleration loggers. *Endang. Spec. Res.* **10**, 71-82. doi:10.3354/esr00247

Whitney, N. M., Lear, K. O., Gaskins, L. C. and Gleiss, A. C. (2016). The effects of temperature and swimming speed on the metabolic rate of the nurse shark (*Ginglymostoma cirratum*, Bonaterre). *J. Exp. Mar. Biol. Ecol.* **477**, 40-46. doi:10.1016/j.jembe.2015.12.009

Whitney, N. M., Lear, O., Gleiss, A. C., Payne, N. and White, C. F. (2018). Advances in the application of high–resolution biologgers to elasmobranch fishes. In *Shark Research: Emerging Technologies and Applications for the Field and Laboratory* (ed. J. C. Carrier, M. R. Heithaus and C. A. Simpfendorfer), pp. 45-70. Boca Raton, FL: CRC Press.

Wieser, W. and Kaufmann, R. (1998). A note on interactions between temperature, viscosity, body size and swimming energetics in fish larvae. *J. Exp. Biol.* **201**, 1369-1372.

Wilson, R. P., White, C. R., Quintana, F., Halsey, L. G., Liebsch, N., Martin, G. R. and Butler, P. J. (2006). Moving towards acceleration for estimates of activity–specific metabolic rate in free–living animals: the case of the cormorant. *J. Anim. Ecol.* **75**, 1081-1090. doi:10.1111/j.1365-2656.2006.01127.x

Wilson, R. P., Börger, L., Holton, M. D., Scantlebury, D. M., Gómez-Laich, A., Quintana, F., Rosell, F., Graf, P. M., Williams, H., Gunner, R. et al. (2020). Estimates for energy expenditure in free–living animals using acceleration proxies: a reappraisal. *J. Anim. Ecol.* **89**, 161-172. doi:10.1111/1365-2656.13040

Wright, S., Metcalfe, J. D., Hetherington, S., Wilson, R. (2014). Estimating activity-specific energy expenditure in a teleost fish, using accelerometer loggers. *Mar. Ecol. Prog. Ser.* **496**, 19-32. doi:10.3354/meps10528

Zuur, A. F., Ieno, E. N., Walker, N. J., Saveliev, A. A. and Smith, G. M. (2009). *Mixed Effects Models and Extensions in Ecology with R*. New York: Spring Science and Business Media.

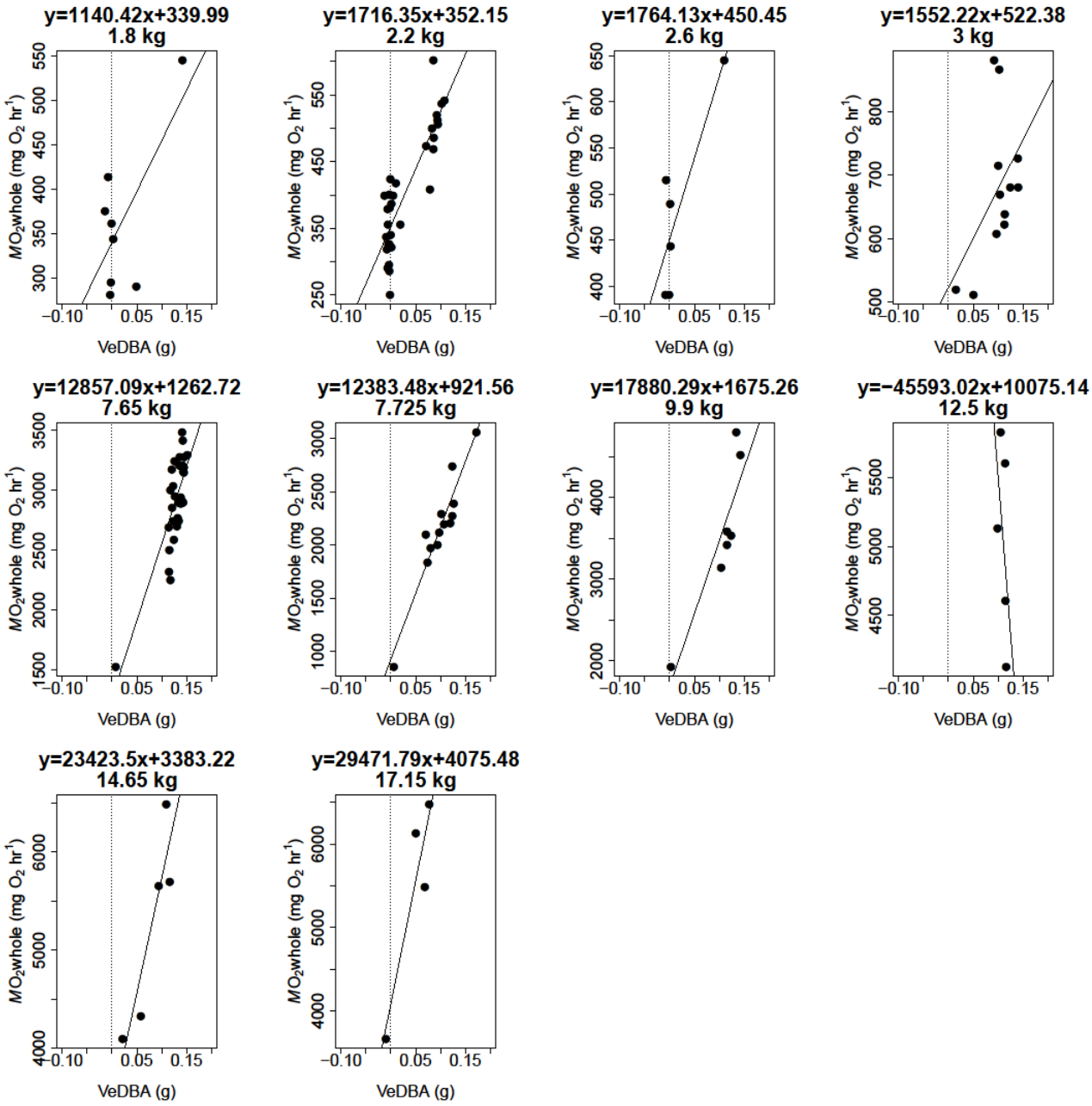

Fig. S1. Linear fits of the $\dot{M}O_{2whole}$-VeDBA relationship for each mass class, predicted by the best-fit linear effects model. The mass and equation for each mass class are shown above the respective plot. Horizontal dotted lines represent the point of zero activity (y-axis).

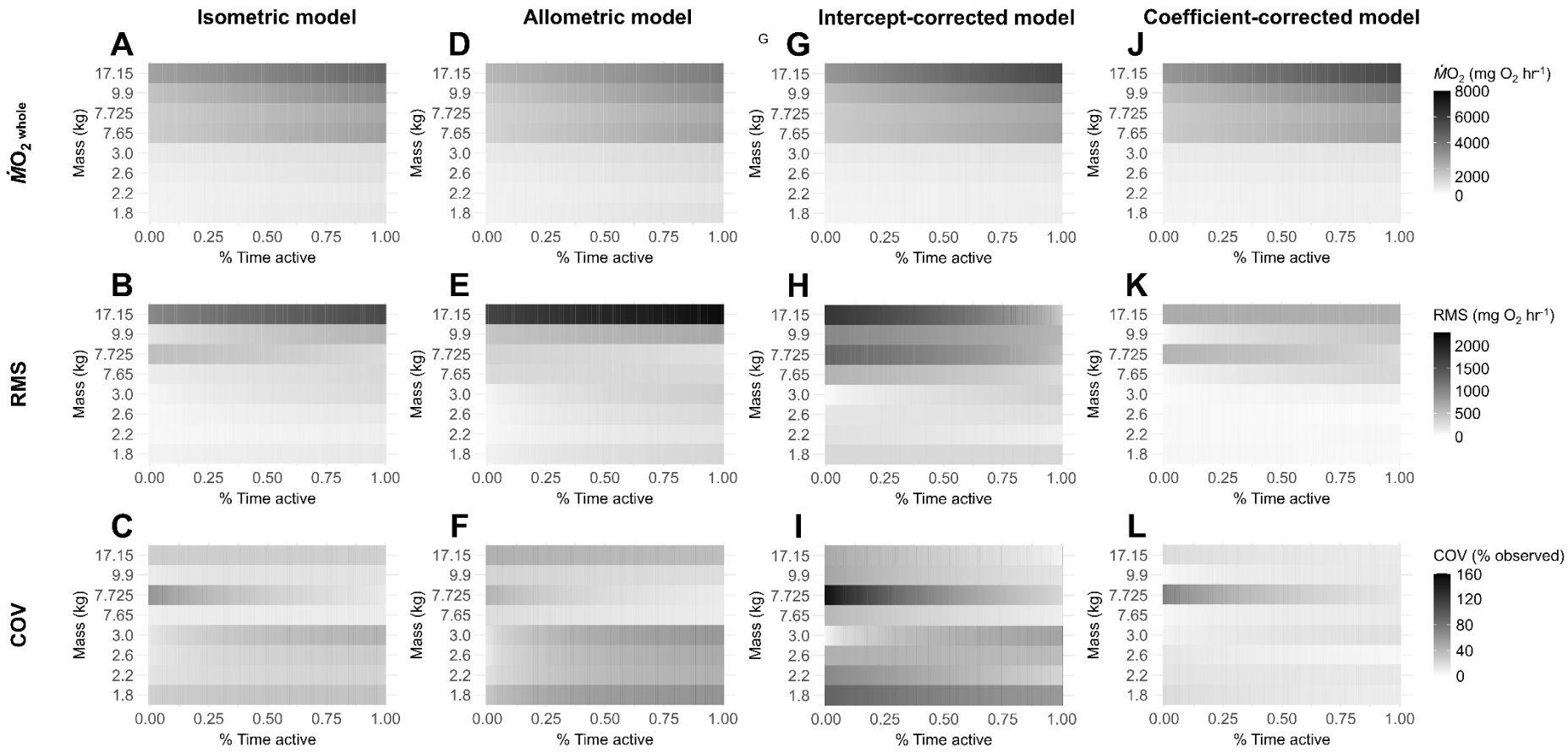

Fig. S2. Results of a simulation conducted to show how estimation error of different whole animal respiration rate ($\dot{M}O_{2whole}$) modelling techniques changes across a range of activity levels and all available mass classes. A day in the life of 100 sharks for all available mass classes (1.8 – 17.15 kg) was repeatedly simulated, where the proportion of time spent active was varied. $\dot{M}O_{2whole}$, root-mean squared error (RMS),

and coefficient of variation (COV) were calculated over the full range of activity for each body mass using the *isometric response-corrected* (A-C), *allometric response-corrected* (D-F), *intercept-corrected* (G-I), and *coefficient-corrected* (J-K) modelling approaches. Resultant values $\dot{M}O_{2whole}$, RMS, COV are colour-coded with low to high values represented by a light to dark gradient, respectively.